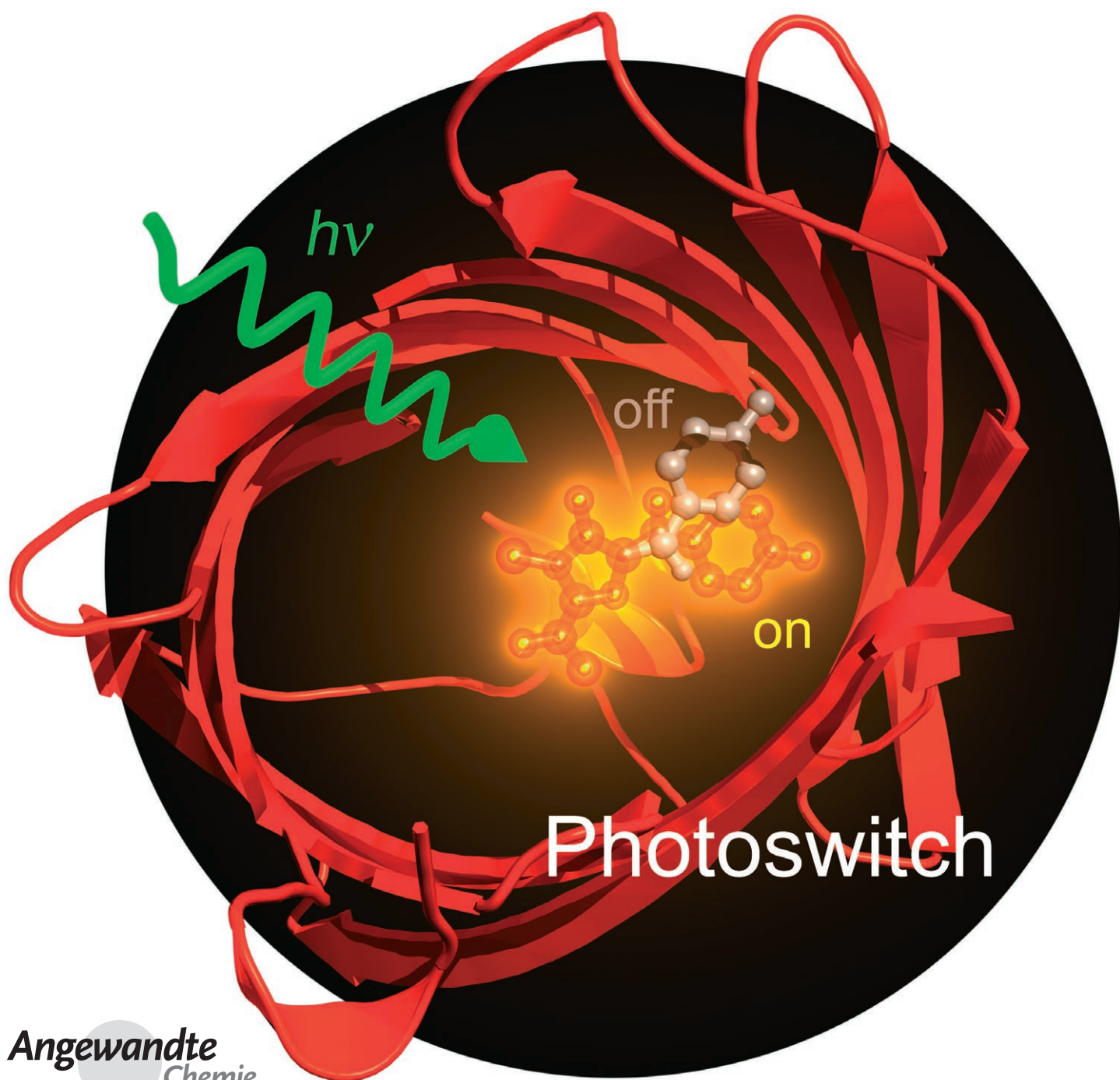


Photoswitching of the Fluorescent Protein asFP595: Mechanism, Proton Pathways, and Absorption Spectra**

Lars V. Schäfer, Gerrit Groenhof, Astrid R. Klungen, G. Matthias Ullmann, Martial Boggio-Pasqua, Michael A. Robb, and Helmut Grubmüller*



Fluorescent proteins have been widely used as genetically encodable fusion tags to monitor protein localization and dynamics in living cells.^[1–3] Recently, a new class of green fluorescent protein (GFP) like proteins has been discovered, which can be reversibly photoswitched between a fluorescent “on” and a nonfluorescent “off” state.^[4–6] As the reversible photoswitching of photochromic organic molecules, such as fulgides or diarylethenes, is usually not accompanied by fluorescence,^[7] this switching reversibility is a very remarkable and unique feature that may allow fundamentally new applications. Hence, not surprisingly, these proteins hold great promise in many areas of science beyond their prominent use as triggerable markers in live cells. For example, the reversible photoswitching, also known as kindling, may provide nanoscale resolution in far-field fluorescence optical microscopy much below the diffraction limit—a break-through hardly imaginable until very recently.^[8–10] Since fluorescence can be sensitively read out from a bulky crystal, the prospect of erasable three-dimensional data storage is equally intriguing.

The GFP-like protein asFP595, isolated from the sea anemone *Anemonia sulcata*, is a prototype for such a photo-switchable protein. It is structurally and spectroscopically well characterized,^[11] but its detailed mechanism remains largely unknown. In particular, it is unclear to what extent associated proton-transfer events determine the optical properties of the chromophore and, if they do, what their pathways are.

The protein asFP595 can be switched from its nonfluorescent “off” state with an absorption maximum at 2.18 eV (568 nm) to the fluorescent “on” state by irradiation with green light. From this so-called kindled on state, red fluorescence emission is elicited by the same green light. Upon kindling, the absorption at 2.18 eV diminishes, and an absorption peak at 2.79 eV (445 nm) appears. This peak was tentatively attributed to the absorption of a different protonation state.^[12] However, the nature of this state is unknown.

Eventually, asFP595 reverts back thermally to the off state. This transition can also be triggered by irradiation with

2.79 eV blue light.^[6] The switching cycle can be repeated many times, a fact rendering asFP595 a promising fluorescence marker for optical microscopy.^[13] Currently, however, with a low quantum yield (<0.1%^[6]) and rather slow switching kinetics, the photochromic properties of asFP595 leave much room for improvement. To systematically exploit the potential of such switchable proteins and to enable rational improvements to the properties of asFP595, a detailed molecular understanding of the switching process is mandatory.

Recently, high-resolution crystal structures of wild-type (wt) asFP595 in its off state,^[11,14,15] of the Ser158Val mutant in its on state, and of the Ala143Ser mutant in its on and off states^[11] were determined. Similarly to GFP, the globular asFP595 adopts a β -barrel fold, which encloses the chromophore, a 2-acetyl-5-(*p*-hydroxybenzylidene)imidazolinone (Figure 1), which is posttranslationally formed in an autocatalytic cyclization and oxidation of the Met63–Tyr64–Gly65 (MYG) triad. Spectroscopic data strongly suggest that the photoswitching of asFP595 is accompanied by protonation-

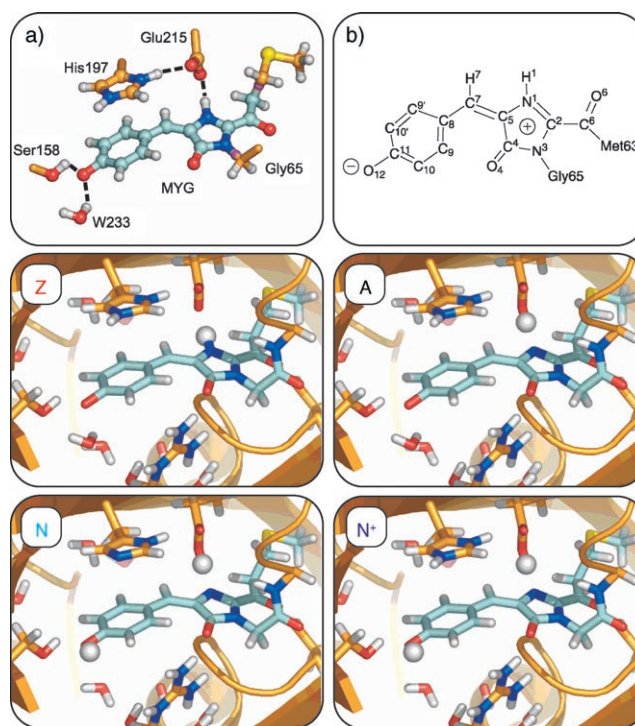


Figure 1. Zwitterionic asFP595 chromophore (MYG) in the dark-state *trans* conformation. a) MYG and adjacent side chains of binding-pocket residues. Glu215, Ser158, and the crystallographic water molecule W233 are hydrogen bonded to MYG, and His197 is π stacked with respect to the MYG phenolate moiety. Color code: carbon skeleton of the QM subsystem used in the QM/MM calculations (see the *Experimental Section*) in turquoise, MM carbon atoms in orange, nitrogen atoms in blue, oxygen atoms in red, sulfur atoms in yellow, and the hydrogen link atoms capping the QM subsystem in magenta. b) Schematic drawing of MYG, defining the atom names used in the text. The protonation states of the chromophore pocket in asFP595 considered in the present study are a zwitterionic state (Z), an anionic state (A), and a neutral state, with His197 singly (N) or doubly protonated (N⁺). Hydrogen atoms characterizing the protonation states are highlighted as spheres.

[*] L. V. Schäfer, Dr. G. Groenhof, Prof. Dr. H. Grubmüller
 Abteilung für theoretische und computergestützte Biophysik
 Max-Planck-Institut für Biophysikalische Chemie
 Am Fassberg 11, 37077 Göttingen (Germany)
 Fax: (+49) 551-201-2302
 E-mail: hgrubmu@gwdg.de

A. R. Kligen, Prof. Dr. G. M. Ullmann
 Abteilung Strukturbiologie/Bioinformatik
 Universität Bayreuth
 Universitätsstrasse 30, 95447 Bayreuth (Germany)

Dr. M. Boggio-Pasqua, Prof. Dr. M. A. Robb
 Department of Chemistry
 Imperial College London
 London SW7 2AZ (UK)

[**] We thank Martin Andresen, Christian Eggeling, Stefan Hell, Stefan Jakobs, Andre Stiel, and Markus Wahl for kindly providing us with the mutant asFP595 structures prior to publication and for stimulating discussions. A.R.K. and L.V.S. thank the Boehringer Ingelheim Fonds for PhD scholarships. We thank Martin Stumpe for his help with the frontispiece.

Supporting information for this article is available on the WWW under <http://www.angewandte.org> or from the author.

state changes of the chromophore.^[12] Additional evidence comes from the related GFP, where proton-transfer processes dominate photoswitching. In GFP, an anionic and a neutral chromophore protonation state are interconverted through a proton-relay mechanism.^[16–20] As protons are not observed in the X-ray crystal structures, their role and possible transfers during the kindling of asFP595 remain largely unclear.

To clarify the role of the protons in the switching mechanism, we have calculated the optical absorption spectra from molecular dynamics (MD) ensembles of a series of asFP595 protonation states, shown in Figure 1. To this end, the semiempirical ZINDO method^[21,22] and time-dependent density functional theory (TDDFT)^[23–27] were employed. In particular, TDDFT has been used to predict absorption energies for a wide variety of biological chromophores, including GFP.^[28–32] Recently, single-structure TDDFT calculations on a small subsystem of asFP595 have been attempted,^[33] with inconclusive results.

Since the spectra of biological chromophores can be strongly tuned by their protein environment, we performed the TDDFT calculations within the quantum mechanics/molecular mechanics (QM/MM) approach.^[34] The chromophore was treated quantum-mechanically, whereas the rest of the system was described at the force-field level (Figure 1 a). To properly account for the protein environment in the ZINDO calculations, the complete chromophore binding pocket was treated at the quantum level (see the Experimental Section). Comparison of the calculated UV/Vis spectra to the available experimental data, in conjunction with computed protonation probabilities of the titratable groups in the chromophore cavity, would allow us 1) to unambiguously assign the protonation patterns of the off and on states of wt asFP595 and 2) to provide atomistic insights into the proton transfers that interconvert the protonation states involved in photoswitching.

Figure 2 shows the UV/Vis spectra for the considered chromophore protonation states of asFP595, defined in Figure 1, calculated at the semiempirical ZINDO level. The absorption spectra computed at the TDDFT level show the same order of states as the semiempirical spectra of Figure 2, although the absolute absorption energies for the anionic and zwitterionic states are blue-shifted too much (see the Supporting Information). Examination of the molecular orbitals revealed that, for all cases, the dominant excitations are $\pi \rightarrow \pi^*$ transitions. For wt asFP595, that is, with the chromophore in the *trans* conformation, the zwitterion (state Z, red curve) displays the most red-shifted absorption, with a strong and narrow maximum at 2.30 eV and a distinct shoulder at 2.41 eV (Figure 2 a).

Transfer of the proton from the imidazolinone nitrogen atom (N1, Figure 1 b) to the Glu215 side chain results in the anionic state A, for which we find a strong absorption band at 2.44 eV, with a shoulder at 2.51 eV (black curve in Figure 2 a). Further protonation of the phenolate oxygen atom (O12, Figure 1 b) leads to the N^+ state and causes a significant blue-shift towards 3.2 eV (blue curve); this absorption band is weaker and much broader than those of the ionic species. The neutral chromophore-state N, with a singly protonated His197, also absorbs at around 3.2 eV (turquoise). A doubly

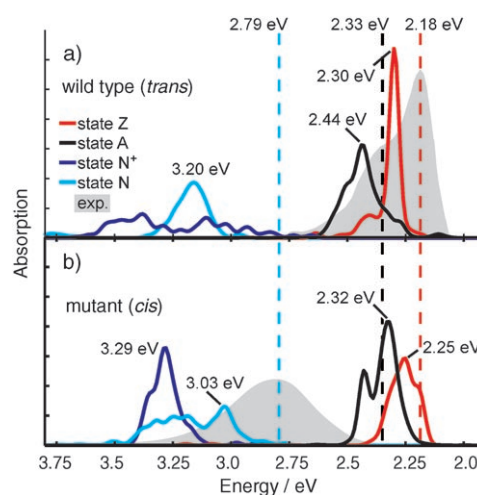


Figure 2. Calculated optical absorption spectra of the asFP595 protonation states shown in Figure 1 for the wt protein (a) and the *cis* mutant (b). The measured absorption spectrum is shown in gray with the maxima indicated by dashed lines. Upon kindling, the zwitterionic and anionic absorptions at 2.18 eV and 2.33 eV, respectively, are depleted, concomitant with a rising peak at 2.79 eV (dashed turquoise line). The experimental spectrum was adopted from reference [12].

anionic state with a negative chromophore and a deprotonated Glu215 was not considered because the close contact between the chromophore and the Glu215 side chain observed in the crystal structure (2.7 Å) requires a hydrogen bond, as shown in the Supporting Information.

To reveal the effect of *trans*–*cis* isomerization on the absorption characteristics of asFP595, we calculated the spectra not only for the wt protein but also for a mutant, whose crystal structure shows density for both the *cis* and *trans* chromophores (Figure 2 b). For all protonation states, the absorption of the *cis* isomer is slightly red-shifted by about 0.05–0.2 eV with respect to that of the *trans* isomer, a fact that is in agreement with recent experiments.^[35] Therefore, the *trans*–*cis* isomerization alone, without concomitant protonation-state changes, cannot explain the observed blue-shift from 2.18 eV to 2.79 eV upon kindling.

As the chromophore of the wt adopts the *trans* conformation in the crystal structure,^[11,14,15] a comparison of the calculated absorption spectra of the *trans* wt (Figure 2 a) with the experimental spectrum allows us to assign the protonation state of the chromophore cavity in wt asFP595. Under physiological conditions, asFP595 has a measured sharp absorption maximum at 2.18 eV and a shoulder which is blue-shifted by 0.15 eV at 2.33 eV (gray curve in Figure 2 a).^[12] Taken together, the calculated sharp maximum of the zwitterion at 2.30 eV and the weaker and broader band of the anion at 2.44 eV yield a spectrum that is only slightly blue-shifted with respect to the measured one (by 0.12 eV). In particular, the oscillator strengths and peak shapes are in good agreement with the experimental spectrum, and the calculated energy difference of 0.14 eV between the zwitterionic and anionic absorption maxima is very accurate. These results suggest that the zwitterion is the dominant species under physiological conditions and that the anion leads to the

observed shoulder in the absorption spectrum. Additional support for this assignment comes from the measured absorption spectrum of the anionic asFP595 chromophore in aqueous solution, which has a maximum at 2.38 eV.^[36]

In both the *trans* and the *cis* conformations, the neutral chromophore absorption is considerably blue-shifted as compared with that of the ionic species at 3.20 eV (*trans*) and 3.03 eV (*cis*). Upon kindling, a rising peak is observed at 2.79 eV (dashed turquoise line in Figure 2), which within the estimated accuracy of the ZINDO calculations (see below) we assign to a population of the neutral *cis* species. The TDDFT spectra support this assignment (see the Supporting Information). Our results suggest that the *trans*–*cis* isomerization of the chromophore is accompanied by protonation-state changes and that the absorbing species populated upon kindling is the neutral *cis* chromophore.

To elucidate the electrostatic and steric effects of the protein environment on the absorption energies, we studied the absorption characteristics in vacuo, both for the molecular dynamics (MD) ensembles and for optimized structures (see the Supporting Information). Both effects slightly blue-shift the absorption energies of the zwitterion and the anion as compared to the gas phase. However, these shifts do not change the order of the absorption bands and thus have no influence on the protonation-state assignment.

We calculated the absorption energies of an anionic and a neutral state of a GFP model chromophore, which is very similar to MYG, to assess the accuracy of the ZINDO and TDDFT methods for asFP595 (see the Supporting Information). We found that the red-shifted absorption of the ionic species is well described at the ZINDO level, whereas TDDFT is more accurate for the neutral species. As ZINDO apparently performs better than TDDFT for the red-shifted absorption regime of asFP595 (around 2.18 eV), we based our protonation-state assignment in this regime on the ZINDO spectra only. For the more blue-shifted regime (around 2.78 eV), both spectra were taken into account.

As an independent check of the protonation-state assignment, we computed the protonation probabilities of all titratable groups in the asFP595 protein by Poisson–Boltzmann electrostatics (PBE). These calculations also predict the zwitterion to be the dominant state for the *trans* chromophore in wt asFP595 under physiological conditions, thereby confirming our assignment based on the UV/Vis spectra. The populations of the states Z, N, and A are about 96, 3, and 1%, respectively. Recently, Schüttrigkeit and co-workers studied asFP595 spectroscopically.^[35] Together with static quantum-chemical calculations of the chromophore in vacuo, their experiments suggest either the anion or the zwitterion to be the protonation state under physiological conditions but cannot distinguish between the two. By taking into account both the chromophore environment as well as dynamic effects for the calculation of the absorption spectra, and by performing PBE calculations, our calculations strongly suggest the zwitterion to be the dominant species.

To study the effect of *trans*–*cis* isomerization on the protonation pattern in the chromophore-binding cavity, we repeated the PBE calculations for both the *trans* and *cis* crystal structures of the mutant. In the mutant, the *trans*

isomer is also zwitterionic (population about 99%), which provides further support for the wt results. For the *cis* conformer, by contrast, the calculations suggest that not the Z but rather the N and A states are equally populated under physiological conditions. However, in the crystal of the mutant, the *cis* chromophore is populated to only a minor degree. The weak electron density obtained for the *cis* structure allowed the assignment of alternative conformations, as compared to the *trans* structure, only for the chromophore and a few additional residues. Therefore, to allow the protein matrix to relax further in response to *trans*–*cis* isomerization, we have repeated the PBE calculations on a *cis* mutant structure that has been energy minimized with positional restraints on all heavy protein atoms (force constant: 1000 kJ mol⁻¹ nm⁻²). In this slightly relaxed environment, the *cis* chromophore adopts the neutral state with a population of 92%, while the anionic and zwitterionic states are populated to only 6 and 2%, respectively. Thus, *trans*–*cis* isomerization is accompanied by a change in protonation pattern from zwitterionic to neutral, although the anionic *cis* state might be accessible under physiological conditions as well.

Minimization of the *trans* structure prior to the PBE calculations had no effect on the preferred protonation state of the chromophore. However, His197 was predicted to be doubly protonated in the minimized structure, whereas the calculations from the X-ray crystal structure predicted it to be singly protonated. This suggests that the actual protonation state of His197 depends critically on the local environment in the chromophore pocket. We therefore cannot unambiguously assign the protonation state of this residue. Most probably, both singly and doubly protonated states are populated under physiological conditions. A cationic His197 could stabilize a partially negatively charged chromophore phenolate ring and might therefore be favored in the zwitterionic and anionic states.

The different populations of the protonation states in the *trans* and *cis* conformations are due to the higher acidity of the zwitterionic imidazolinone NH proton in the *cis* isomer compared to that in the *trans* isomer. Our density functional calculations estimated p*K* values of 4.7 and 9.1 for the *cis* and *trans* chromophores in aqueous solution, respectively (see the Supporting Information). This shift of about 4.4 p*K* units is due to steric repulsion between the NH hydrogen atom and one of the phenolate *ortho* protons because these are forced into closer proximity in the *cis* isomer.

In summary, the PBE results corroborate that the chromophore *trans*–*cis* photoisomerization upon kindling of asFP595 is accompanied by proton-transfer events. After or during isomerization, a proton is transferred from the imidazolinone ring of the zwitterion to Glu215, thereby yielding the anionic chromophore. Since the calculations revealed the neutral chromophore (state N) to be the most stable species in the *cis* conformation, the anion is probably a metastable intermediate that is readily protonated at the phenolate oxygen atom to give the neutral *cis* chromophore.

Combination of the calculated optical absorption spectra and the results of the PBE allows us to proceed further and to address the mechanism of asFP595 kindling in detail. We will

focus on the proton wires mediating the interconversion of the chromophore protonation states.

The proposed kindling mechanism is depicted in Figure 3. As shown previously, kindling is initiated by a *trans*–*cis* photoisomerization through a space-saving hula-twist mechanism.^[11] The isomerization increases the acidity of the

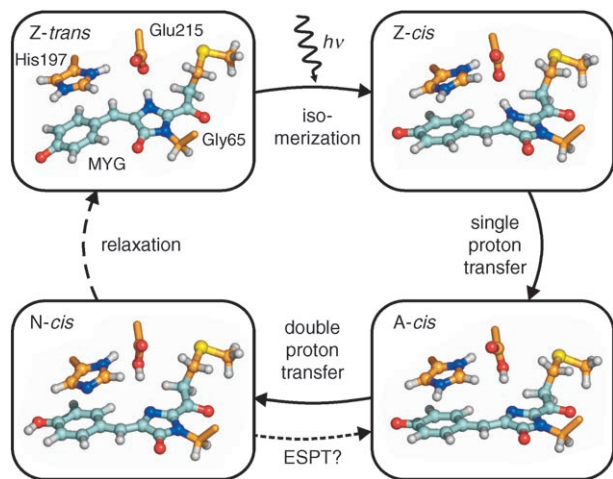


Figure 3. Proposed kindling mechanism of asFP595. For details see text. Atom colors are the same as in Figure 1.

imidazolinone NH proton of the zwitterionic *cis* chromophore and induces proton transfer to Glu215 (state *A-cis*, Figure 3). Whether this proton transfer takes place in the electronic ground state or in the excited state cannot be judged on the basis of the current simulations. The proton transfer also prevents photoisomerization of the zwitterionic *cis* species back to the initial dark *trans* state. The anionic *cis* intermediate is subsequently protonated at the phenolate oxygen atom to finally yield the stable neutral chromophore (state *N-cis*). This situation is similar to that in GFP, where the neutral protonation state is also favored for the *cis* chromophore.^[16–20] GFP fluorescence originates from the anionic chromophore, which is formed through excited-state proton transfer (ESPT). Further studies are required to elucidate whether such ESPT processes play an important role in asFP595 as well.

Protonation of the anion requires a proton donor in close proximity to the phenolate oxygen atom. Figure 1 shows that, intuitively, His197 could provide the proton, but it seems to be too far away for a direct proton transfer. To address this issue, we performed a 20-ns force-field MD simulation of the anionic *cis* state and identified relevant hydrogen bonds (data not shown). His197 does not form a hydrogen bond to the chromophore in the course of the simulation due to their coplanar arrangement (Figure 1). Instead, a stable hydrogen bond is seen between His197 and Glu145 (see Figure 4), which therefore might serve as a proton shuttle. However, proton shuttling would additionally require a chain of two or three water molecules to be established between Glu145 and the phenolate oxygen atom O12, which was not observed in either the MD simulation or in the X-ray crystal structure.

Figure 4 suggests an alternative protonation pathway. Close examination of the simulations revealed that protons in the chromophore pocket could exchange with protons in the bulk through two distinct proton wires connecting the pocket

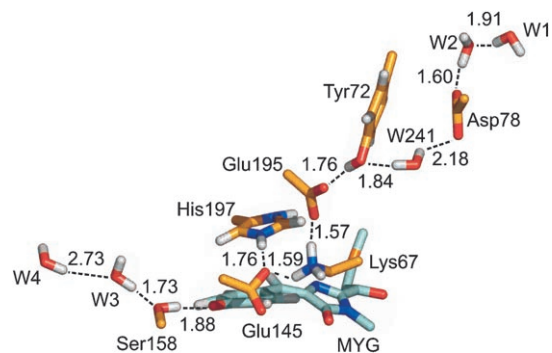


Figure 4. Snapshot from an MD simulation showing the proposed proton-entry and -release wires in asFP595. Color code: carbon atoms of MYG in turquoise and of the amino acid side chains involved in the proton wires in orange, oxygen atoms in red, nitrogen atoms in blue. Aliphatic hydrogen atoms are not shown. The distances between the proton-donor and -acceptor atoms are given in Å.

to the exterior solution. These wires involve several protonatable side chains and one buried crystallographic water molecule. The proton entrance pathway involves Ser158, which is directly hydrogen bonded to the phenolate oxygen atom of the chromophore. In the simulations, this residue is connected to the bulk solution through a short chain of water molecules (W3 and W4, Figure 4), thereby enabling proton uptake by the chromophore from the solvent. In the X-ray crystal structure, the water molecule W233 (Figure 1 a) is also hydrogen bonded to the phenolate oxygen atom and could therefore also be involved.

The putative proton-release pathway of the His197 proton starts at Glu145 and proceeds through Lys67, Glu195, and Tyr72 towards Asp78. The crystal water molecule W241 temporarily bridges Tyr72 and Asp78 in the simulation, as shown in Figure 4. Located on the surface of the protein, Asp78 finally releases the proton to the exterior solution. The hydrogen-bonded network remained intact during the simulations, such that the donor and acceptor distances were always optimal for proton transfer. It is known from quantum dynamics simulations^[37] that the rate of proton migration along such wires is dominated by tunneling, suggesting that the proton exchange occurs by rapid one-dimensional diffusion^[18,19] of protons along the two wires.

The kindling mechanism at the atomic level can be summarized as follows: After photon absorption, the dark zwitterionic *trans* state of the chromophore is converted into an anion state by a proton transfer from the imidazolinone moiety to the side chain of Glu215. This process could either happen after or during *trans*–*cis* isomerization. A short wire involving Ser158 and a crystallographic water molecule connects the chromophore cavity to the exterior solution and mediates the subsequent protonation of the anionic phenolate oxygen atom, thereby finally leading to the *cis*

neutral form of the chromophore. Proton release from the doubly protonated His197 into the exterior solution proceeds along an extended proton wire involving five residues and a buried water molecule.

This kindling mechanism is remarkably similar to the fluorescence mechanism of GFP, in that their chromophores are neutral in the *cis* ground-state conformation. In both asFP595 and GFP the chromophore is connected to the exterior solution by proton wires, which mediate the protonation-state changes. These similarities suggest that proton transfers might also be essential for a mechanistic understanding of other fluorescent proteins. Indeed, it was shown recently that photoswitching of the GFP-like proteins Dronpa,^[38] DsRed,^[39] and EosFP^[40] involves protonation-state changes of the chromophore as well. However, for all three cases, the molecular mechanisms and proton pathways remain to be elucidated at the atomic level.

Furthermore, the similarities should enable one to exploit the broad range of mutants that have already been characterized for GFP to improve the fluorescence of asFP595. For example, a residue with a higher proton affinity could be introduced near the phenolate oxygen atom of the chromophore to enhance the formation of the anionic species. Also tempting is the observation that, in contrast to asFP595, GFP has an internal proton-relay mechanism that efficiently shuttles the proton from the phenolate oxygen atom to a nearby glutamic acid. This, together with the presence of similar proton wires,^[18] suggests that the introduction of a similar internal relay mechanism might also improve the fluorescence of asFP595.

The conformational flexibility of the asFP595 chromophore is, in contrast to that of GFP, sufficiently high to allow *trans-cis* isomerization which triggers a proton transfer cascade, preventing the immediate re-isomerization to the initial dark state induced by a second photon. Other photoactive proteins have also evolved mechanisms to avoid the immediate photochemical back-reaction. As in asFP595, such mechanisms require that the initial photoproduct is not the most stable ground-state minimum, but rather an intermediate in the overall process. Photoisomerization leading to changes in the protonation probabilities is also known as the critical step in the signal-transduction mechanism of bacteriorhodopsin^[41] and photoactive yellow protein.^[42,43] The quite different structures of these three examples suggest that evolution has exploited this idea as a general principle.

Experimental Section

The UV/Vis spectra were calculated in three steps. First, extensive classical MD simulations for five different protonation states of the chromophore pocket of wt asFP595 and of a *cis* mutant structure were performed to generate thermodynamic ensembles. The five protonation states covered all conceivable chromophore protonation states: the zwitterionic state “Z”, an anionic state “A”, a neutral state “N⁺”, a neutral state “N”, and a double-anionic state “D”. A doubly protonated cationic chromophore was not considered due to its high acidity.^[47] After minimization and equilibration, each system was simulated for 7.5 ns. The starting coordinates for the simulations were taken from the 1.3 Å X-ray crystal structure (Protein Data Bank (PDB) entry 2A50^[11]). All simulations were performed by using the

Gromacs simulation package^[48] together with the OPLS all-atom force field.^[49] For details of the simulations, see the Supporting Information.

Second, for each protonation state, a sufficient number of structures (100 equidistant frames extracted from each force-field trajectory) were extracted and modestly relaxed (very short QM/MM geometry optimizations (HF/3-21G*, ONIOM)). Finally, the excitation energies were calculated for these relaxed structures and superimposed. In the QM/MM TDDFT calculations, the chromophore was described quantum mechanically at the TD-BVP86/6-31G* level of theory,^[44–46] and the rest of the protein, water molecules, and ions were described at the force-field level (Figure 1 a). In the ZINDO calculations, the majority of the chromophore-binding pocket, composed of the entire MYG chromophore and the side chains of residues Lys67, Arg92, Glu145, Ser158, His197, and Glu215, and the crystallographic water molecule W233 were described at the quantum chemical level. All QM/MM TDDFT calculations were performed with Gromacs 3.3 software^[48] and its QM/MM interface^[43] to the Gaussian03 program.^[50] Modifications were made in the one-electron integral routines of Gaussian03 for the TDDFT computations of the chromophore polarized by gaussian charge distributions of the MM atoms. For details, see the Supporting Information.

Spectra were composed from the calculated absorption energies ΔE_{ji}^{\max} by superposition of Gaussian functions [Eq. (1)]. Here, ΔE_{ji}^{\max}

$$G(\Delta E) = \sum_{i=1}^{100} \sum_{j=1}^3 f_{ji} \exp \left[-\frac{(\Delta E - \Delta E_{ji}^{\max})^2}{2\sigma^2} \right] \quad (1)$$

are the excitation energies of the first three excited singlet states ($j=1,2,3$) of structure i , and f_{ji} is the corresponding oscillator strength. A width of $\sigma=0.02$ eV was chosen.

To quantify the population of the different protonation states of the chromophore pocket, PBE calculations^[51] were performed on wt asFP595 (PDB entry 2A50^[11]) and the mutant structure, which shows density for both the *cis* and *trans* chromophores. This allowed the effect of the *trans-cis* photoisomerization on the protonation states of the chromophore pocket to be evaluated. Protonation probabilities were calculated with the MEAD program package^[52] and a Metropolis Monte Carlo algorithm to sample protonation-state energies.^[53] See the Supporting Information for details of the Poisson–Boltzmann calculations.

Received: June 9, 2006

Revised: September 8, 2006

Published online: November 9, 2006

Keywords: absorption spectroscopy · isomerization · molecular dynamics · proteins · proton transport

- [1] J. Lippincott-Schwartz, N. Altan-Bonnet, G. H. Patterson, *Nat. Cell Biol.* **2003**, *Suppl. S*, 7.
- [2] A. Miyawaki, A. Sawano, T. Kogure, *Nat. Cell Biol.* **2003**, *Suppl. S*, 1.
- [3] R. Y. Tsien, *Annu. Rev. Biochem.* **1998**, *67*, 509.
- [4] R. Ando, H. Mizuno, A. Miyawaki, *Science* **2004**, *306*, 1370.
- [5] D. M. Chudakov, V. V. Belousov, A. G. Zarisky, V. V. Novoselov, D. B. Staroverov, D. B. Zorov, S. Lukyanov, K. A. Lukyanov, *Nat. Biotechnol.* **2003**, *21*, 191.
- [6] K. A. Lukyanov, A. F. Fradkov, N. G. Gurskaya, M. V. Matz, Y. A. Labas, A. P. Savitsky, M. L. Markelov, A. G. Zaraisky, X. N. Zhao, Y. Fang, W. Y. Tan, S. A. Lukyanov, *J. Biol. Chem.* **2000**, *275*, 25879.
- [7] *Organic Photochromic and Thermochromic Compounds: Main Photochromic Families, Vol. 1* (Eds.: J. C. Crano, R. J. Gugliemetti), Plenum, New York, **1999**.

- [8] S. W. Hell, S. Jakobs, L. Kastrup, *Appl. Phys. A* **2003**, *77*, 859.
- [9] S. W. Hell, *Nat. Biotechnol.* **2003**, *21*, 1347.
- [10] S. W. Hell, M. Dyba, S. Jakobs, *Curr. Opin. Neurobiol.* **2004**, *14*, 599.
- [11] M. Andresen, M. C. Wahl, A. C. Stiel, F. Gräter, L. V. Schäfer, S. Trowitzsch, G. Weber, C. Eggeling, H. Grubmüller, S. W. Hell, S. Jakobs, *Proc. Natl. Acad. Sci. USA* **2005**, *102*, 13070.
- [12] D. M. Chudakov, A. V. Feofanov, N. N. Mudrik, S. Lukyanov, K. A. Lukyanov, *J. Biol. Chem.* **2003**, *278*, 7215.
- [13] M. Hofmann, C. Eggeling, S. Jakobs, S. W. Hell, *Proc. Natl. Acad. Sci. USA* **2005**, *102*, 17565.
- [14] P. G. Wilmann, J. Petersen, R. J. Devenish, M. Prescott, J. Rossjohn, *J. Biol. Chem.* **2005**, *280*, 2401.
- [15] M. L. Quillin, D. A. Anstrom, X. K. Shu, S. O'Leary, K. Kallio, D. A. Chudakov, S. J. Remington, *Biochemistry* **2005**, *44*, 5774.
- [16] V. Helms, *Curr. Opin. Struct. Biol.* **2002**, *12*, 169.
- [17] D. Stoner-Ma, A. A. Jaye, P. Matousek, M. Towrie, S. R. Meech, P. J. Tonge, *J. Am. Chem. Soc.* **2005**, *127*, 2864.
- [18] N. Agmon, *Biophys. J.* **2005**, *88*, 2452.
- [19] P. Leiderman, D. Huppert, N. Agmon, *Biophys. J.* **2006**, *90*, 1009.
- [20] O. Vendrell, R. Gelabert, M. Moreno, J. M. Lluch, *J. Am. Chem. Soc.* **2006**, *128*, 3564.
- [21] A. D. Bacon, M. C. Zerner, *Theor. Chim. Acta* **1979**, *53*, 21.
- [22] L. K. Hanson, J. Fajer, M. A. Thompson, M. C. Zerner, *J. Am. Chem. Soc.* **1987**, *109*, 4728.
- [23] L. N. Oliveira, E. K. U. Gross, W. Kohn, *Int. J. Quant. Chem.* **1990**, *Suppl. 24*, 707.
- [24] E. Runge, E. K. U. Gross, *Phys. Rev. Lett.* **1984**, *52*, 997.
- [25] *Recent Advances in Density Functional Methods* (Eds.: M. E. Casida, D. P. Chong), World Scientific Publishing, Singapore, **1995**.
- [26] M. Petersilka, U. J. Gossmann, E. K. U. Gross, *Phys. Rev. Lett.* **1996**, *76*, 1212.
- [27] C. Jamorski, M. E. Casida, D. R. Salahub, *J. Chem. Phys.* **1996**, *104*, 5134.
- [28] G. Groenhof, M. F. Lensink, H. J. C. Berendsen, J. G. Snijders, A. E. Mark, *Proteins Struct. Funct. Genet.* **2002**, *48*, 202.
- [29] M. A. L. Marques, X. Lopez, D. Varsano, A. Castro, A. Rubio, *Phys. Rev. Lett.* **2003**, *90*, 2581011.
- [30] J. A. Gascon, V. S. Batista, *Biophys. J.* **2004**, *87*, 2931.
- [31] X. Lopez, M. A. L. Marques, A. Castro, A. Rubio, *J. Am. Chem. Soc.* **2005**, *127*, 12329.
- [32] N. Sanna, G. Chillemi, A. Grandi, S. Castelli, A. Desideri, V. Barone, *J. Am. Chem. Soc.* **2005**, *127*, 15429.
- [33] B. Grigorenko, A. Savitsky, I. Topol, S. Burt, A. Nemukhin, *Chem. Phys. Lett.* **2006**, *424*, 184.
- [34] A. Warshel, M. Levitt, *J. Mol. Biol.* **1976**, *103*, 227.
- [35] T. A. Schüttrigkeit, T. von Feilitzsch, C. K. Kompa, K. A. Lukyanov, A. P. Savitsky, A. A. Voityuk, M. E. Michel-Beyerle, *Chem. Phys.* **2006**, *323*, 149.
- [36] I. V. Yampolsky, S. J. Remington, V. I. Martynov, V. K. Potapov, S. Lukyanov, K. A. Lukyanov, *Biochemistry* **2005**, *44*, 5788.
- [37] A. Warshel, *Proc. Natl. Acad. Sci. USA* **1984**, *81*, 444.
- [38] S. Habuchi, R. Ando, P. Dedecker, W. Verheijen, H. Mizuno, A. Miyakawa, J. Hofkens, *Proc. Natl. Acad. Sci. USA* **2005**, *102*, 9511.
- [39] S. Habuchi, M. Cotlet, T. Gensch, T. Bednarz, S. Haber-Pohlmeier, J. Rozenski, G. Dirix, J. Michiels, J. Vanderleyden, J. Heberle, F. C. DeSchryver, J. Hofkens, *J. Am. Chem. Soc.* **2005**, *127*, 8977.
- [40] G. U. Nienhaus, K. Nienhaus, A. Holzle, S. Ivanchenko, F. Renzi, F. Oswald, M. Wolff, F. Schmitt, C. Rucker, B. Vallone, W. Weidemann, R. Heilker, H. Nar, J. Wiedenmann, *Photochem. Photobiol.* **2006**, *82*, 351.
- [41] B. Bieger, L.-O. Essen, D. Oesterhelt, *Structure* **2003**, *11*, 375.
- [42] N. M. Derix, R. W. Wechselberger, M. A. van der Horst, K. J. Hellingwerf, R. Boelens, R. Kaptein, N. A. J. van Nuland, *Biochemistry* **2003**, *42*, 14501.
- [43] G. Groenhof, M. Bouxin-Cademartory, B. Hess, S. P. de Visser, H. J. C. Berendsen, M. Olivucci, A. E. Mark, M. A. Robb, *J. Am. Chem. Soc.* **2004**, *126*, 4228.
- [44] S. H. Vosko, L. Wilk, M. Nusair, *Can. J. Phys.* **1980**, *58*, 1200.
- [45] A. D. Becke, *Phys. Rev. A* **1988**, *38*, 3098.
- [46] J. P. Perdew, *Phys. Rev. B* **1986**, *33*, 8822.
- [47] A. F. Bell, X. He, R. M. Wachter, P. J. Tonge, *Biochemistry* **2000**, *39*, 4423.
- [48] D. van der Spoel, B. Hess, E. Lindahl, G. Groenhof, A. E. Mark, H. J. C. Berendsen, *J. Comput. Chem.* **2005**, *26*, 1701.
- [49] W. L. Jorgensen, J. Tirado-Rives, *J. Am. Chem. Soc.* **1988**, *110*, 1657.
- [50] Gaussian 03, M. J. Frisch, G. W. Trucks, H. B. Schlegel, G. E. Scuseria, M. A. Robb, J. R. Cheeseman, J. A. Montgomery, Jr., T. Vreven, K. N. Kudin, J. C. Burant, J. M. Millam, S. S. Iyengar, J. Tomasi, V. Barone, B. Mennucci, M. Cossi, G. Scalmani, N. Rega, G. A. Petersson, H. Nakatsuji, M. Hada, M. Ehara, K. Toyota, R. Fukuda, J. Hasegawa, M. Ishida, T. Nakajima, Y. Honda, O. Kitao, H. Nakai, M. Klene, X. Li, J. E. Knox, H. P. Hratchian, J. B. Cross, C. Adamo, J. Jaramillo, R. Gomperts, R. E. Stratmann, O. Yazyev, A. J. Austin, R. Cammi, C. Pomelli, J. W. Ochterski, P. Y. Ayala, K. Morokuma, G. A. Voth, P. Salvador, J. J. Dannenberg, V. G. Zakrzewski, S. Dapprich, A. D. Daniels, M. C. Strain, O. Farkas, D. K. Malick, A. D. Rabuck, K. Raghavachari, J. B. Foresman, J. V. Ortiz, Q. Cui, A. G. Baboul, S. Clifford, J. Cioslowski, B. B. Stefanov, G. Liu, A. Liashenko, P. Piskorz, I. Komaromi, D. J. Fox, T. Keith, M. A. Al-Laham, C. Y. Peng, A. Nanayakkara, M. Challacombe, P. M. W. Gill, B. Johnson, W. Chen, M. W. Wong, C. Gonzalez, J. A. Pople, Gaussian, Inc., Pittsburgh, PA, **2003**.
- [51] G. M. Ullmann, E.-W. Knapp, *Eur. Biophys. J.* **1999**, *28*, 533.
- [52] D. Bashford, M. Karplus, *Biochemistry* **1990**, *29*, 10219.
- [53] QMCT: a Monte Carlo titration program, G. M. Ullmann, Universität Bayrouth, **2005**.